Reviews on Advanced Materials and Technologies, 2026, vol. 8, no. 1, pp. 15–21
DOI: 10.17586/2687-0568-2026-8-1-15-21

Composition Undulation Induced Strain Hardening in Fine-Grained FCC Alloys

A.G. Sheinerman [1,2,*]

[1] Institute for Problems in Mechanical Engineering, Russian Academy of Sciences, Bolshoi pr., V.O., 61, St. Petersburg 199178, Russia
[2] Saint Petersburg State University, Universitetskaya nab., 7/9, St. Petersburg, 199034 Russia

Article history

Received November 24, 2025
Accepted December 03, 2025
Available online March 12, 2026

Abstract

A model is suggested that describes tensile plastic deformation of fine-grained FCC alloys with three-dimensional composition undulation. Within the model, composition undulation is approximated by spherical inclusions, which envelope the region of highest and lowest solute concentration. It is assumed that these inclusions can increase the yield strength due to their misfit stresses and, in addition, initiate the cross-slip of screw dislocations that otherwise tend to move in a planar mode. The initiation of additional dislocation slip systems reduces the dislocation mean slip path, which increases the dislocation density, enhances strain hardening and thereby increases the ultimate strength and ductility of alloys. It is demonstrated that the maximum ultimate strength can be achieved either at low or at high values of the composition undulation wavelength, while the uniform elongation slightly decreases with an increase in the composition undulation wavelength.

Keywords: Alloys; Composition modulation; Strength; Ductility

1. INTRODUCTION

Achieving a combination of ultra-high strength and high tensile ductility is a critical challenge in the design of modern structural materials [1,2]. Face-centered cubic (FCC) alloys, including high-entropy alloys (HEAs) and medium-entropy alloys (MEAs), are used in many engineering applications due to their inherent strength and promising strain-hardening capabilities [3,4]. However, traditional strengthening mechanisms, such as grain refinement or precipitation strengthening, often significantly reduce ductility, leading to a long-standing trade-off between strength and ductility [2,5]. To overcome this limitation, studies have been conducted on chemical heterogeneities at the nanoscale level within a single-phase solid solution. One type of such heterogeneities is composition undulation, which represents continuous, quasi-periodic spatial fluctuations in atomic concentration [1,5].

Composition undulations create an oscillating lattice strain field that roughens the dislocation slip path without introducing sharp interphase boundaries [6]. The most effective method for generating these undulations is through spinodal decomposition, a phase separation mechanism that occurs spontaneously within the spinodal region of a thermodynamically unstable solid solution [6]. In HEAs and MEAs, this process can be controlled via aging to produce undulations with wavelengths typically ranging from a few to tens of nanometers [7]. Recent studies have demonstrated that composition undulations can also be created through electrochemical dealloying [8] or additive manufacturing [9].

The impact of composition undulation on strength and ductility has been demonstrated for several alloy classes. An example is the NiCo solid solution, where engineered composition undulations resulted in a significant increase in the ultimate strength while preserving substantial uniform elongation [1]. Similarly, composition undulations were studied for other systems, such as refractory HEAs (e.g., Ti-Zr-Hf-Nb system), where spinodally decomposed structures suppress brittle failure [7].

* Corresponding author: A.G. Sheinerman, e-mail: asheinerman@gmail.com

The mechanisms of strengthening associated with composition undulations incorporate the interaction of dislocations with misfit stresses, their motion in the varying stacking fault energy landscape [1], and dislocation interactions and tangling, which are enhanced by composition undulations [5,10–12]. This can promote the generation of dislocation networks and thereby resist the strain localization that typically leads to early necking and failure [13]. Recent studies have confirmed that composition undulations can allow the material to activate additional plasticity mechanisms, such as transformation-induced plasticity (TRIP), at high stress levels, further delaying failure [14,15].

Recently, we have studied the combined effect of composition undulations on the yield strength increase due to the misfit stresses and stacking fault energy variation and strain hardening associated with the formation of sessile dislocations at the dislocation pinning points [16]. However, it was demonstrated [17] that in FCC alloys, dislocation pinning points can also initiate cross-slip of screw dislocations, leading to the activation of multiple slip systems followed by an abrupt decrease in the dislocation mean slip and increase in strain hardening. The aim of the present paper is to theoretically study the effect of misfit stresses and dislocation cross-slip associated with composition undulations in fcc alloys on their strain hardening, strength and ductility.

2. MODEL

Consider a plastically deformed annealed fine-grained alloy with three-dimensional composition undulation. We examine the situation where composition undulation is isotropic. In the case where composition undulation is caused by spinodal decomposition, this means that there no preferable directions for the decomposition. In this case, the regions of highest or lowest solute concentration are spherical. For this situation, following Ref. [16], we neglect the heterogeneity of the solute concentration both inside and outside such regions and approximate these regions as coherent spherical inclusions with a constant concentration of solutes located in an infinite matrix with another constant concentrations of solute atoms. For this case, the average radius of the model inclusions can be related to their volume fraction V_i and the wavelength λ as [16]: $\overline{r} = [3V_i / (32\pi)]^{1/3} \lambda$.

The difference between the concentrations of solute atoms inside and outside the inclusions leads to a difference (misfit) in the lattice parameters of the matrix and inclusions and, as a consequence, creates misfit stresses that elastically interact with moving dislocations during plastic deformation of the alloy. The misfit f that defines the relative difference in the crystal lattice parameters of inclusions and the matrix can be defined as $f = (1/a_m)(\partial a/\partial c)\Delta c$, where a_m is the crystal lattice parameter of the matrix, and a is the crystal lattice parameter of the solid solution, which depends on the solute concentration c, and Δc is the amplitude of the composition undulation. For simplicity, here we neglect the effect of the difference in the elastic moduli of the matrix and inclusions and model the matrix and inclusions as elastically isotropic regions with the same elastic constants (shear modulus G and Poisson's ratio ν).

It is known (e.g., Ref. [18]) that the contribution of the inclusions to the yield strength does not depend on the sign of the misfit. Therefore, hereafter, we will not distinguish between the inclusions that encompass the regions of the highest and smallest solute concentration and will treat all of them as being characterized by the misfit f.

Now consider a plastically deformed fine-grained alloy with composition undulation approximated by an ensemble of spherical inclusions, subjected to a uniaxial tensile load. We focus on the typical case where the stress for inclusion shearing is smaller than that for the formation of Orowan loops. However, we assume that in some cases, screw dislocations retarded at inclusions can cross-slip. We assume that this is possible if the critical applied load for the shearing of an inclusion by a screw dislocation is higher than that for the dislocation cross-slip. Since in the examined case of misfit-induced strengthening, the critical stress for inclusion shearing by a screw dislocation is much smaller than that for a mixed or edge dislocation, the contribution of screw dislocations to the yield strength enhancement σ_i associated with inclusions is small compared to those of mixed and edge dislocations. Therefore, in the following we neglect the effect of dislocation cross-slip on the yield strength. Then the stress σ_i can be presented as [18]

$$\sigma_i = 2.6\sqrt{2} M G f^{3/2} (\overline{r} V_i / b)^{1/2}, \quad (1)$$

where $\overline{r}$ is the average inclusion radius, M is the Taylor factor, equal to 3.06 for FCC crystals, and b is the magnitude of the dislocation Burgers vector.

3. FLOW STRESS OF ALLOYS WITH COMPOSITION UNDULATION

Now let us calculate the flow stress of an alloy with composition undulation, where the principle mechanism of plastic deformation is the motion of lattice dislocations. The expression for the true flow stress σ_f can be presented as

$$\sigma_f = \sigma_0 + \sigma_i + \sigma_d, \quad (2)$$

where σ_0 is the term taking into account the lattice friction, the interaction of dislocations with the solid solution and the presence of grain boundaries, and σ_d is the term that describes the strengthening due to the forest dislocations. The stress σ_d associated with the forest dislocations is calculated as (e.g., Refs. [19–22])

$$\sigma_d = \alpha M G b \sqrt{\rho(\varepsilon_p)}, \quad (3)$$

where α is a numerical factor and $\rho(\varepsilon_p)$ is the forest dislocation density at the true plastic strain ε_p.

To calculate the flow stress, the Taylor formula given by Eq. (3) should be combined with the equation describing the evolution of the dislocation density in the course of plastic deformation. If the grain size exceeds several nanometers, so that the effect of grain boundaries on the dislocation slip path can, as a rule, be neglected, the equation for the evolution of the dislocation density is given by [23]

$$\frac{d\rho}{d\varepsilon_p} = M\left(\frac{k_1}{b}\sqrt{\rho} - k_2\rho\right). \quad (4)$$

In formula (4), the parameters k_1 and k_2 determine the rate of dislocation multiplication and annihilation, respectively, and k_1 is related to the dislocation mean slip distance $\overline{l}$ as $\overline{l} \approx 1/(k_1\sqrt{\rho})$.

In the following, we focus on the case where in the absence of inclusions, dislocations slip in a planar manner. This case is typical for FCC alloys with a relatively small stacking fault energy. We assume that inclusions induce the cross-slip of screw dislocations and the activation of multiple slip systems, which results in the abrupt decline in the dislocation mean slip path (e.g., Ref. [17]). This implies that cross-slipped dislocations increase the value of k_1. In addition, dislocation cross-slip can also increase the probability of dislocation annihilation, which leads to an increase in the value of k_1. However, in what follows we assume that for annealed fine-grained alloys, the dislocation density is relatively small, and a change in the term $k_2\rho$ (associated with increased dislocation annihilation) in formula (4) is small compared to the change in the term $(k_1/b)\sqrt{\rho}$ (related to the decline in the dislocation mean slip path) in this formula. In this case, the effect of enhanced dislocation annihilation (associated with dislocation cross-slip) on the parameter k_2 can be neglected.

Let k_1^s represent the limiting value of the parameter k_1 for the model case where all dislocations are screw, while k_1^0 denote the limiting value of the parameter k_2 in the model situation where screw dislocations are absent (so that any dislocation is either edge or mixed). We suppose that in the absence of inclusions, the mean path of screw, edge and mixed dislocations is the same, that is, $k_1^s = k_1^0$. We also assume that in the case where inclusions are present, the value of the parameter k_1 can be obtained using the mixture rule as $k_1 = hk_1^s + (1-h)k_1^0$, where h is the proportion of screw dislocations. Next, we assume that the quantity k_1^s linearly scales with the number of cross-slipped dislocations. Assuming that the dislocation slip distance obeys an exponential distribution, the probability that a moving screw dislocation encounters an inclusion at which it can cross-slip is equal [24] to $\exp\left(-l_0/\overline{l}\right)$, where l_0 is the average distance from the initial position of a moving dislocation to the inclusion edge, which is approximated here by the distance between the centers of those inclusions in the dislocation slip plane at which screw dislocations can cross-slip. Within this approximation, one can put $\overline{l} \approx 1/(k_1\sqrt{\rho}) \approx 1/(k_1^0\sqrt{\rho})$. Then we have

$$k_1^s(\rho) = k_1^0\left(1 - e^{-k_1^0\sqrt{\rho}l_0}\right) + k_1^p e^{-k_1^0\sqrt{\rho}l_0}, \quad (5)$$

where k_1^p is the parameter that characterizes the mean slip distance in the limiting case where all dislocations cross-slip. The distance l_0 is given [25] by $l_0 = \overline{r}\sqrt{2\pi/(3V_iP)}$. Here P is the fraction of inclusions where screw dislocations are favored to cross-slip.

To calculate P, we assume that a screw dislocation that encounters an inclusion of radius r is favored to cross-slip if the average critical applied stress σ_s for the inclusion shearing by a screw dislocation is larger than the critical applied stress σ_{cs} for dislocation cross-slip ($\sigma_s > \sigma_{cs}$). In the following, we neglect the effect of the inclusion stresses on σ_{cs} and assume that σ_{cs} does not depend on the inclusion radius and volume fraction. The stress σ_s for the shearing of an inclusion of radius r by a screw dislocation can be obtained from the formulae presented in Ref. [18] as

$$\sigma_s = AGf^{3/2}\left(\frac{rV_i}{b}\right)^{1/2}\left(\frac{r}{\overline{r}}\right)^{3/2}, \quad (6)$$

where A is a numerical factor. Using formula (6), we can rewrite the condition $\sigma_s > \sigma_{cs}$ as $r > r_c$, where

$$r_c = \sqrt{\frac{\sigma_{cs}\overline{r}^{3/2}b^{1/2}}{AGf^{3/2}V_i^{1/2}}}. \quad (7)$$

Now suppose that the radius r of inclusions obeys the lognormal distribution with the distribution density [26]

$$\rho_{distr}(r) = \frac{1}{r\sqrt{2\pi s^2}}\exp\left[-\frac{(\ln(r/\overline{r}) + s^2/2)^2}{2s^2}\right], \quad (8)$$

where s is the dispersion of $\ln r$. Then the fraction P of inclusions where screw dislocations are favored to cross-slip is equal to the probability that $\sigma_s > \sigma_{cs}$. The expression for P has the form

$$P = \int_{r_c}^{\infty} \rho_{distr}(r)\,dr. \quad (9)$$

Formulae (5) and (7)–(9) combined with the expression $l_0 = \overline{r}\sqrt{2\pi/(3V_iP)}$ enables one to obtain the explicit expression for the right-hand side of formula (4). The solution to equation (4) follows as:

$$\varepsilon_p(\rho) = \frac{b}{M}\int_{\rho_0}^{\rho}\frac{d\rho'}{k_1(\rho')\sqrt{\rho'} - bk_2\rho'}, \quad (10)$$

where ρ_0 is the initial dislocation density. Together with formulae (2) and (3) that relate the flow stress with the

dislocation density ρ, formula (10) provides the relation between the true flow stress σ_f and true plastic strain ε_p.

The total true strain ε of a plastically deformed alloy is equal to the sum of the elastic strain σ_f / E (where $E = 2G(1+\nu)$ is the Young modulus of the alloy) and the plastic strain ε_p: $\varepsilon = \sigma_f / E + \varepsilon_p$. The true stresses and strains can be related to the engineering stress σ_e and engineering strain ε_e as $\varepsilon_e = e^{\varepsilon} - 1$ and $\sigma_e = \sigma_f / (1+\varepsilon_e)$.

Now consider the case where the solid fails due to necking. In this case, the onset of necking instability is described by the Considère criterion [27]

$$\partial\sigma_f / \partial\varepsilon = \sigma_f. \quad (11)$$

Taking into account that $\partial\sigma_f / \partial\varepsilon \approx \partial\sigma_f / \partial\varepsilon_p = \frac{\partial\sigma_f}{\partial\rho}\frac{\partial\rho}{\partial\varepsilon_p}$ and substituting the latter relation and formulae (2)–(4) to formula (11), one obtains the following relation describing the onset of necking: $\rho = \rho_c$, where the critical dislocation density ρ_c can be found from the equation

$$\alpha GbM\sqrt{\rho_c}\,(2 + Mk_2) = \alpha GM^2 k_1(\rho_c) - 2(\sigma_0 + \sigma_i). \quad (12)$$

The onset of necking instability defines the engineering uniform elongation ε_c, which describes the value of the engineering strain ε_e at which necking instability appears. Also, the onset of necking instability corresponds to the maximum at the dependence $\sigma_e(\varepsilon_e)$, which determines the engineering ultimate strength σ_B. Therefore, the ultimate strength σ_B and uniform elongation ε_c follow as $\sigma_B = \sigma_e(\rho = \rho_c)$ and $\varepsilon_c = \varepsilon_e(\rho = \rho_c)$. Although uniform elongation is smaller than strain to failure, in the following we will use this parameter to characterize ductility of alloys.

4. RESULTS AND DISCUSSION

Now we calculate the stress σ_e for the case of the FCC $Fe_{61.75}Ni_{14.25}Co_{7.6}Mn_{7.6}Ti_{2.85}Si_{0.95}Cu_{4.5}Al_{0.5}$ medium entropy alloy, hereafter denoted as Fe MEA, where strengthening associated with the composition undulation has recently been observed experimentally [28]. We characterize this alloy by the following parameter values [28]: G = 78.4 GPa, f = 0.376%, b = 0.2548 nm. We also put α = 0.3, V_i = 0.2, s = 0.5, h = 0.5, $\rho_0 = 0$, $\sigma_{cs} / A = 15$ MPa and $\bar{r} = 2$ nm, which corresponds in the examined case V_i = 0.2 to the observed [28] undulation wavelength λ = 11 nm. The quantities of k_1^0, k_1^p, k_2 and σ_0 are taken as fitting parameters, and their values are set as follows: $k_1^0 = 0.03$, $k_1^p = 0.08$, $k_2 = 7.5$, $\sigma_0 = 840$ MPa for the aged Fe MEA with composition undulation and $\sigma_0 = 590$ MPa for the same unaged Fe MEA without composition undulation. The reason for using different values of σ_0 for the aged and unaged alloy is the formation of precipitates due to aging in work [28], which increase the yield strength and whose formation is not explicitly accounted for in our model.

The calculated dependences of the engineering stress σ_e on the engineering strain ε_e for the Fe MEA with the above parameter values are shown in Fig. 1a by solid lines. Here the red solid curve corresponds to the Fe MEA with composition undulation, while the blue solid curve describes the Fe MEA without composition undulation. The corresponding experimental curves from Ref. [28] are depicted in Fig. 1a by the red and blue dotted lines. It is seen in Fig. 1a that the calculated curves, which are plotted until the point of the onset of necking instability, satisfactorily agree with the experimental curves.

The dependences $\sigma_e(\varepsilon_e)$ for the Fe MEAs characterized by various values of the average inclusion radius $\bar{r}$ and a constant value of σ_0 (σ_0 = 840 MPa), which is taken here the same for the alloys with composition undulation and without it, are displayed in Fig. 1b. Figure 1b demonstrates that the flow stress increases with an increase in $\bar{r}$, which is associated with an increase in the yield strength. In the examined case of a relatively high misfit (f = 0.376%), the contribution of the inclusions misfit stresses to the yield strength (and to the ultimate strength) are dominant, while the effect of the inclusion-related strain hardening

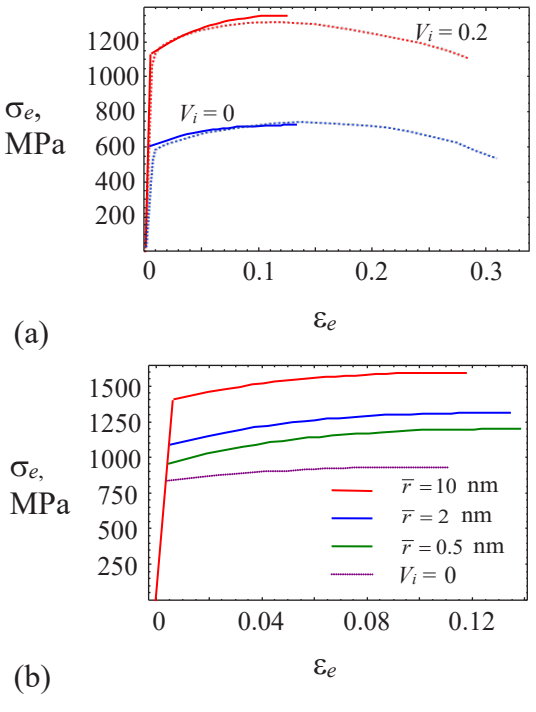

Fig. 1. Dependences of the engineering stress σ_e on the engineering strain ε_e for the case of uniaxial tension of the Fe MEA. (a) The red and blue lines show the cases of the Fe MEA with composition undulation (V_i = 0.2, red lines) and without composition undulation (V_i = 0, blue lines). The solid lines illustrate the calculated dependences, while the dashed lines show the experimental dependences from Ref. [28]. Average inclusion radius is $\bar{r}$ = 2 nm. (b) The calculated dependences for different values of the average inclusion radius $\bar{r}$ (solid curves) and V_i = 0.2. The purple dotted curve depicts the case where composition undulation is absent (V_i = 0).

on the flow stress is smaller. The comparison of the curves $\sigma_e(\varepsilon_e)$ for the case of composition undulation with the case where composition undulation is absent demonstrates that composition undulation, in addition to increasing the yield strength, enhances strain hardening. The right end of the curves in Fig. 1b show the values of the ultimate strength σ_B and uniform elongation ε_c. It is seen in Fig. 1b that the ultimate strength increases due to the composition undulation, while the uniform elongation can either increase or decrease, depending on the value of $\overline{r}$.

Figure 2 illustrates the dependences of the ultimate strength σ_B of the Fe MEA on the average inclusion radius $\overline{r}$ for two various values of misfit f and various values of the parameter k_1^p that determines the effect of inclusions on strain hardening. It follows from Fig. 2 that in the case of a relatively high misfit ($f = 0.376\%$), the ultimate strength σ_B increases with $\overline{r}$, similarly to the flow stress σ_e (see Fig. 1b). In contrast, for a smaller value of misfit ($f = 0.1\%$), the situation can be different (Fig. 2b). In this case, for a small value of k_1^p ($k_1^p = 0.05$), when the strain hardening effect of inclusions is relatively small, the effect of the inclusion misfit stresses on the ultimate strength is still higher than the effect related to the inclusion-induced increase in strain hardening.

For this case, the ultimate strength σ_B monotonously increases with $\overline{r}$. At the same time, for higher values of k_1^p, the strain hardening effect of inclusions on the ultimate strength can be comparable to that of the inclusion misfit stresses. In this situation, σ_B first decreases and then increases with $\overline{r}$, and a high ultimate strength can be achieved in the case of either a low or a high inclusion radius, which corresponds to either a low or a high composition undulation wavelength. An increase in the ultimate strength with a decrease in $\overline{r}$ at relatively small values of $\overline{r}$ is associated with an increase in the number density of inclusions. (At a specified volume fraction of inclusions, when inclusions become smaller, their number increases.) A higher number of inclusions leads to higher strain hardening. In turn, enhanced strain hardening increases the ultimate strength. With an increase in $\overline{r}$, strain hardening effect of inclusion decays (due to a decrese in their number), while the contribution of the inclusion misfit stresses to the ultimate strength grows in accord with formula (1). As a result, the effect of the inclusion misfit stresses on the ultimate strength starts to prevail over their strain hadening effect. This leads to the transition from a decrease to an increase of the ultimate strength σ_B with a growth of $\overline{r}$.

The uniform elongation ε_c is presented in Fig. 3 as a function of the average inclusion radius $\overline{r}$, for $f = 0.1\%$ and various values of k_1^p. Figure 3 demonstrates that ε_c increases with a decrease of $\overline{r}$ due to both lower yield strength and enhanced strain hardening. In addition, ε_c increases with an increase in k_1^p, which is also related to higher strain hardening.

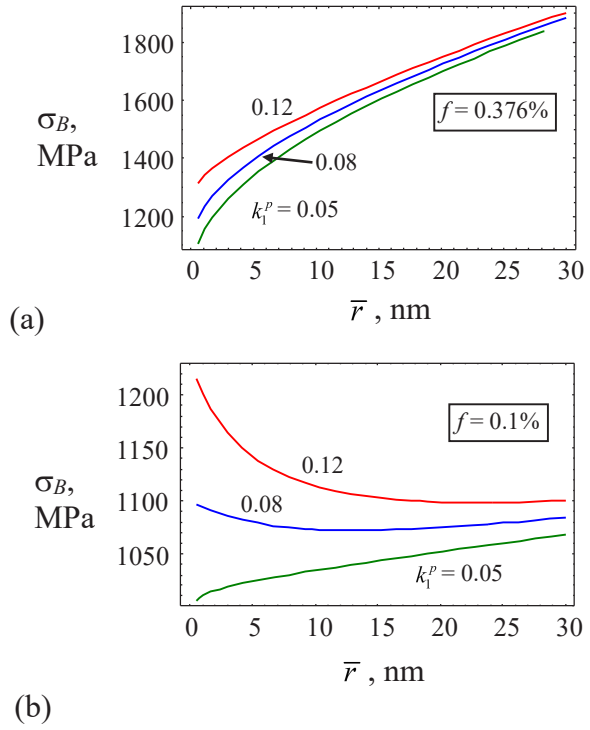

Fig. 2. Dependences of the ultimate tensile strength σ_B of the Fe MEA on the average inclusion radius $\overline{r}$, for $V_i = 0.2$, various values of the parameter k_1^p, $f = 0.376\%$ (a) and 0.1% (b).

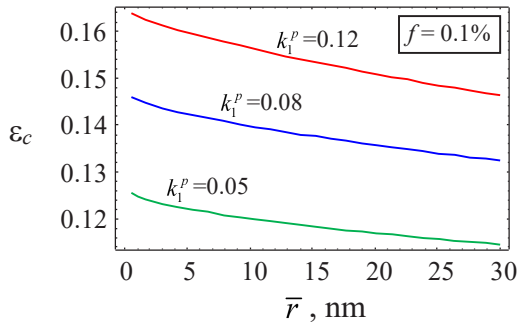

Fig. 3. Dependences of the uniform elongation ε_c of the Fe MEA on the average inclusion radius $\overline{r}$, for $V_i = 0.2$ and various values of the parameter k_1^p.

Thus, the calculations demonstrate that composition undulation can lead not only to the yield strength increase but also to enhanced strain hardening. These two factors differently affect strength and ductility of alloys. An increase in the yield strength due to the inclusion misfit stresses is stronger at a high average inclusion radius (which also implies a high undulation wavelength) and increases the ultimate strength but reduces ductility. Meanwhile, enhanced strain hardening due to the dislocation cross-slip at inclusions is more pronounced at a small average inclusion radius (which also means a small undulation wavelength) and can increase both the ultimate strength and ductility of alloys.

The calculations also demonstrate that if composition undulation can induce significant strain hardening, the

high ultimate strength can be achieved not only at a high, but also at a small undulation wavelength (Fig. 2b), and such a small undulation wavelength will provide higher ductility (Fig. 3).

5. SUMMARY

Thus, we have suggested a model that describes tensile plastic deformation of fine-grained alloys with three-dimensional composition undulation. We examined the case where composition undulation can not only increase the yield strength due to the misfit stresses but also promote the transition from planar to wavy slip, which can decrease the dislocation mean path, thereby increasing stain hardening, yield strength and ductility. It is demonstrated that depending on the values of the misfit f and the parameter k_1^p describing the effect of inclusions on strain hardening, the maximum ultimate strength can be achieved either at low or at high values of the composition undulation wavelength. The uniform elongation can either increase or decrease due to the presence of inclusions and slightly decreases with an increase in the undulation wavelength. The model demonstrates that dislocation cross-slip associated with the composition undulation can increase strain hardening and thereby increase both strength and ductility of alloys.

ACKNOWLEDGEMENTS

The author acknowledges the financial support of the Russian Science Foundation (grant 24-21-00034).

REFERENCES

[1] H. Li, H. Zong, S. Li, S. Jin, Y. Chen, M.J. Cabral, B. Chen, Q. Huang, Y. Chen, Y. Ren, K. Yu, S. Han, X. Ding, G. Sha, J. Lian, X. Liao, E. Ma, J. Sun. Uniting tensile ductility with ultrahigh strength via composition undulation. *Nature*, 2022, vol. 604, pp. 273–279.

[2] R.O. Ritchie. The conflicts between strength and toughness. *Nature Materials*, 2011, vol. 10, pp. 817–822.

[3] E.P. George, D. Raabe, R.O. Ritchie. High-entropy alloys. *Nature Reviews Materials*, 2019, vol. 4, pp. 515–534.

[4] W. Zhang, P.K. Liaw, Y. Zhang. Science and technology in high-entropy alloys. *Science China Materials*, 2018, vol. 61, pp. 2–22.

[5] H. Wang, B.S. Dong, Z.B. Chen, J.Q. Liu, N. Haghdadi, R.Q. Lu, S. Primig, Z.Y. Wang, Z.X. Pan, H.J. Li, S.P. Ringer, X.Z. Liao. Effect of compositional heterogeneity on the mechanical properties of a single-phase Cu–9Al alloy with different grain sizes. *Acta Materialia*, 2024, vol. 263, art. no. 119531.

[6] Z. Li, S. Zhao, R.O. Ritchie, M.A. Meyers. Mechanical properties of high-entropy alloys with emphasis on face-centered cubic alloys. *Progress in Materials Science*, 2019, vol. 102, pp. 296–345.

[7] Z. An, S. Mao, T. Yang, C.T. Liu, B. Zhang, E. Ma, H. Zhou, Z. Zhang, L. Wang, X. Han. Spinodal-modulated solid solution delivers a strong and ductile refractory high-entropy alloy. *Materials Horizons*, 2021, vol. 8, no. 3, pp. 948–955.

[8] H. Guan, H. Xie, Z.-P. Luo, W.-K. Bao, Z.-S. You, Z. Jin, H.-J. Jin. Ultrastrong spinodoid alloys enabled by electrochemical dealloying and refilling. *Proceedings of the National Academy of Sciences of the USA*, 2023, vol. 120, no. 1, art. no. e2214773120.

[9] B. Gwalani, V. Soni, O.A. Waseem, S.A. Mantri, R. Banerjee. Laser additive manufacturing of compositionally graded AlCrFeMoVx (x = 0–1) high-entropy alloy system. *Optics and Laser Technology*, 2019, vol. 113, pp. 330–337.

[10] E. Ma, X. Wu. Tailoring heterogeneities in high-entropy alloys to promote strength–ductility synergy. *Nature Communications*, 2019, vol. 10, art. no. 3563.

[11] Q.J. Li, H. Sheng, E. Ma. Strengthening in multi-principal element alloys with local-chemical-order roughened dislocation pathways. *Nature Communications*, 2019, vol. 10, art. no. 3563.

[12] Q. Ding, Y. Zhang, X. Chen, X. Fu, D. Chen, S. Chen, L. Gu, F. Wei, H. Bei, Y. Gao, M. Wen, J. Li, Z. Zhang, T. Zhu, R.O. Ritchie, Q. Yu. Tuning element distribution, structure and properties by composition in high-entropy alloys. *Nature*, 2019, vol. 574, pp. 223–227.

[13] Y. Ikeda, B. Grabowski, F. Körmann. Ab initio phase stabilities and mechanical properties of multicomponent alloys: A comprehensive review for high-entropy alloys and compositionally complex alloys. *Materials Characterization*, 2019, vol. 147, pp. 464–511.

[14] J. Zhu, L. Sun, D. Li, L. Zhu, X. He. Compositional undulation induced strain hardening and delocalization in multi-principal element alloys. *International Journal of Mechanical Sciences*, 2023, vol. 241, art. no. 107931.

[15] Y.-C. Wu, J.-L. Shao. FCC–BCC phase transformation induced simultaneous enhancement of tensile strength and ductility at high strain rate in high-entropy alloy. *International Journal of Plasticity*, 2023, vol. 169, art. no. 103730.

[16] A.M. Smirnov, A.G. Sheinerman, X.T. Li, Z.J. Zhang. Modeling strength and ductility of alloys with intragrain compositional inhomogeneities. *International Journal of Plasticity*, submitted.

[17] S.-D. Kim, S.-J. Park, J.H. Jang, J. Moon, H.-Y. Ha, C.-H. Lee, H. Park, J.-H. Shin, T.-H. Lee. Strain hardening recovery mediated by coherent precipitates in lightweight steel. *Scientific Reports*, 2021, vol. 11, art. no. 14468.

[18] A.J. Ardell. Precipitation hardening. *Metallurgical Transactions A*, 1985, vol. 16, pp. 2131–2165.

[19] G.I. Taylor. The mechanism of plastic deformation of crystals. Part I. Theoretical. *Proceedings of the Royal Society A*, 1934, vol. 145, pp. 362–387.

[20] Y. Estrin, H. Mecking. A unified phenomenological description of work hardening and creep based on one-parameter models. *Acta Metallurgica*, 1984, vol. 32, no. 1, pp. 57–70.

[21] M.E. Kassner, K. Kyle. Taylor hardening in five power law creep of metals and class M alloys. In: M.A. Meyers, M. Sarikaya, R.O. Ritchie (Eds.). *Nano and Microstructural Design of Advanced Materials*. Elsevier, 2003, pp. 255–271.

[22] W.J. Poole, J.D. Embury, D.J. Lloyd. Work hardening in aluminum alloys. In: R. Lumley (Ed.). *Fundamentals of Aluminum Metallurgy: Production, Processing and Applications*. Woodhead Publishing, 2011, pp. 307–344.

[23] H. Mecking, U.F. Kocks. Kinetics of flow and strain-hardening. *Acta Metallurgica*, 1981, vol. 29, no. 11, pp. 1865–1875.

[24] R. Schouwenaars. Calculating the grain size effect during strain hardening through a probabilistic analysis of the mean slip distance in polycrystals. *International Journal of Plasticity*, 2024, vol. 178, art. no. 104012.
[25] S.V. Bobylev, A.G. Sheinerman, X.T. Li, Z.J. Zhang. Modeling of strength and ductility of metal alloy/graphene composites containing precipitates. *International Journal of Solids and Structures*, 2024, vol. 296, art. no. 112843.
[26] A.A. Fedorov, M.Yu. Gutkin, I.A. Ovid'ko. Triple junction diffusion and plastic flow in fine-grained materials. *Scripta Materialia*, 2002, vol. 47, no. 1, pp. 51–55.
[27] A. Considère. Mémoire sur l'emploi du fer et de l'acier dans les constructions. *Annales des Ponts et Chaussées*, 1885, vol. 9, pp. 574–775.
[28] H. Park, F. Haftlang, Y. Heo, J. Seol, Z. Wang, H. Kim. Periodic spinodal decomposition in double-strengthened medium-entropy alloy. *Nature Communications*, 2024, vol. 15, art. no. 5757.

УДК 538.911

Деформационное упрочнение в мелкозернистых ГЦК сплавах, вызванное неоднородностью состава

А.Г. Шейнерман [1,2]

[1] Институт проблем машиноведения РАН, Большой пр., В.О., 61, 199178, Санкт-Петербург, Россия
[2] Санкт-Петербургский государственный университет Университетская наб., 7/9, 199034, Санкт-Петербург, Россия

Аннотация. Предложена модель, описывающая пластическую деформацию при растяжении мелкозернистых сплавов с ГЦК структурой и трехмерной модуляцией состава. В рамках модели модуляция состава аппроксимируется сферическими включениями, которые охватывают области с наибольшей и наименьшей концентрацией растворенного вещества. Предполагается, что эти включения могут повышать предел текучести за счет напряжений несоответствия и, кроме того, инициировать поперечное скольжение винтовых дислокаций, которые в отсутствие включений движутся в параллельных плоскостях скольжения. Активация дополнительных систем скольжения дислокаций уменьшает среднюю длину скольжения дислокаций, что увеличивает плотность дислокаций, повышает деформационное упрочнение и, следовательно, увеличивает предел прочности и пластичность сплавов. Показано, что максимальный предел прочности может быть достигнут как при низких, так и при высоких значениях длины волны модуляции состава, в то время как величина равномерного удлинения незначительно уменьшается с ростом длины волны модуляции состава.

Ключевые слова: сплавы; модуляция состава; прочность; пластичность